International Journal of Science and Research Archive
eISSN: 2582-8185
Cross Ref DOI: 10.30574/ijsra
Journal homepage: https://ijsra.net/

(RESEARCH ARTICLE)

Check for updates

Speed Control of a Brushless DC Motor Using Rotary Encoder

Airel Dara Swastika * and Slamet Riyadi

Department of Electrical Engineering, Faculty of Engineering, Soegijapranata Catholic University, Semarang, Indonesia.

International Journal of Science and Research Archive, 2026, 18(01), 896-909

Publication history: Received on 13 December 2025; revised on 24 January 2026; accepted on 27 January 2026

Article DOI: https://doi.org/10.30574/ijsra.2026.18.1.0126

Abstract

Electric and hybrid electric vehicles need a drive system with high torque and simple controls. The BLDC (Brushless DC) motor is perfect for these uses and makes it easy to manage the speed. Even though it is quite complicated, it is possible to control the speed of BLDC motors by using accurate current-based regulation. A simple way to control speed is to use the output pulses from a rotary encoder with comparing them to a reference. This paper introduces a simple control system that uses rotary encoder pulses in conjunction with the dsPIC30F4012 controller. The error between the reference speed and the actual speed (measured in rotary encoder pulses) will be examined through hysteresis to provide a switching signal for the BLDC motor driving converter. Simulations and laboratory experiments were conducted to validate the analytical findings. The results of the simulation and testing indicate that the proposed controller operates efficiently.

Keywords: BLDC Motor; Rotary Encoder; Speed Control; Hysteresis Control

1. Introduction

Electric motors are very important for the growing fields of technology and automation, especially in drive systems. BLDC motors are widely used because they have a simple structure, don't need any maintenance, have a high torque, very efficient, and last a long time [1], [2]. It is important to create a precise and adaptable control system in order to get the most out of BLDC motors. In six-step commutation, the rotor's location is shown to the BLDC motor by signals from Hall effect sensors [3]. Particularly at low speeds or in situations requiring precise dynamic control, this method reveals serious problems with the precision and accuracy of speed data. Due to their low resolution, hall sensors provide inaccurate speed feedback and make it difficult to achieve constant and smooth speed control [4].

The problems with hall sensor-based BLDC motor control have been the subject of numerous studies, with a focus on improving speed accuracy and dynamic performance. Previous studies have looked at ways to manage sensorless systems without the need for physical sensors, such as by determining the rotor position using electrical factors such the Back Electromotive Force (BEMF). On the other hand, at low speeds, this tactic failed to produce consistent results [5]. Improving the quality of control became more important as development went on. The hysteresis control was selected because it is easy to install, responds quickly to changes in the load, and does not require complex adjustments to the parameters [6]. This method has been shown to work well in making systems more stable in a wide range of scenarios without the need for exact mathematical models [7]. However, hysteresis control doesn't work as well because hall sensors can't give accurate position feedback.

* Corresponding author: Airel Dara Swastika

This research presents a rotary encoder as an alternative to the conventional hall effect sensor to solve these issues. The encoder gives a speed signal that is substantially more accurate and reliable. This helps the controller figure out the velocity of objects [8]. If it gets the right feedback, a hysteresis control system will better manage the speed of the motor [9]. This will make sure that it works without using complicated control methods that slow down the microcontroller. The goal is to learn how the BLDC motor and the rotary encoder work. Using the dsPIC30F4012 to make a microcontroller-based speed control system. After that, this system will be tested in a lab and through simulations to make sure it works.

The goal of this research is to create a prototype closed-loop speed control system for BLDC motors that uses speed data from a rotary encoder sensor. This method is expected to keep the motor speed at the reference value with more stability and accuracy than a hall effect sensor. The motor with good speed control will keep the output voltage stable even when the setpoint value (reference input) changes. This enhancement makes it easier to make a high-performance BLDC motor control system that is easy to use, advanced, and reliable.

2. Material and methods

2.1. Basic Principle

BLDC motors are a top choice for many modern uses since they work better than other types of motors, especially when it comes to reliability and energy efficiency. This benefit comes directly from the way it is built, which is very different from how most brushed DC motors are built. Structurally, a BLDC motor consists of two main components featuring a stator winding and a rotor made of permanent magnets [10]. Because it doesn't use a commutator brush, the commutation function is taken over by an electronic commutation system using Hall effect sensors integrated inside the motor to detect the rotor's magnetic field. The working principle of the motor is based on the electromagnetic interaction between the rotating magnetic field generated by the stator windings and the constant magnetic field of the rotor permanent magnets [11].

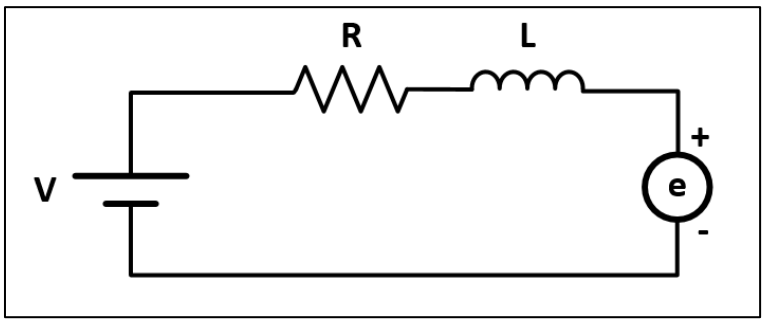

Figure 1 Equivalent circuit of BLDC motor

One cycle of rotation in a BLDC motor is composed of six commutation steps. Unlike mechanical cycles, electrical cycles are determined by the number of poles on the rotor. Rotor position detection is necessary to determine the correct winding excitation sequence, which is typically achieved using three Hall-effect sensors symmetrically mounted on the stator with an electrical angle shift of 120°. The voltage applied to each phase must be shifted by 120° to produce a smooth rotating magnetic field, which is the main operating principle of a BLDC motor [12]. Based on the equivalent circuit of the BLDC motor in Figure 1, the voltage generated by the inverter must overcome the BEMF (e) and the coil impedance. The relationship is formulated.

$$V = iR + L\frac{di}{dt} + e \quad (1)$$

A fundamental component in a BLDC motor drive system is the inverter, which plays a crucial role in power conversion. The inverter's function is to transform the DC input voltage source into a regulated three-phase AC output voltage with controlled amplitude and frequency. The inverter used is a simple three-phase inverter with six active switches, as shown in Figure 2.

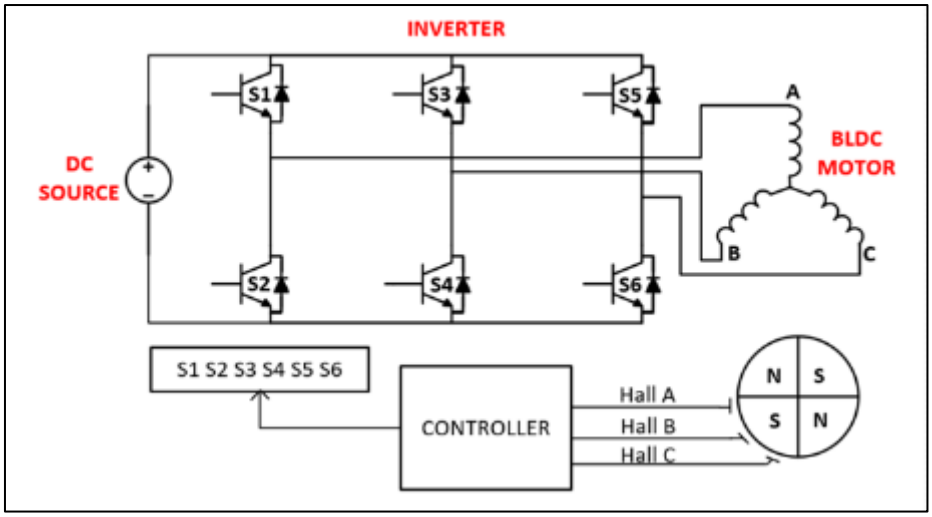

Figure 2 Basic BLDC Motor drive

A three-phase inverter sends voltage to each of the stator phase windings (*A*, *B*, and *C*) while the motor is running. For the motor to operate, the commutation procedure must be done in the right order. The timing of commutation is based on real-time information about the rotor's position. The Hall-effect sensors make a digital signal (high or low) when the rotor's permanent magnet poles pass by them. This signal means that the sensor has found the north or south pole. The correct commutation sequence can be determined by examining the output signals from all three Hall sensors. Table 1 shows the order of commutation.

Table 1 Switching sequence of the three-phase inverter and the resulting motor current flow based on hall effect position feedback

STEP	HALL EFFECT	ON STATE	CURRENT (+)	CURRENT (-)
1	1 0 0	S1-S6	i_a	i_c
2	1 1 0	S3-S6	i_b	i_c
3	0 1 0	S3-S2	i_b	i_a
4	0 1 1	S5-S2	i_c	i_a
5	0 0 1	S5-S4	i_c	i_b
6	1 0 1	S1-S4	i_a	i_b

Each commutation step determines which switches on the inverter must be activated, which in turn controls the direction of current flow into or out of the motor windings. By following the six-step commutation strategy, at each 60° electrical interval, only two of the three phase windings are excited simultaneously [13]. This pattern ensures that one winding carries positive current (current flowing in), one of the remaining two windings carries negative current (current flowing out), while the third winding is in an unexcited (floating) state. The timing diagram of the Hall effect and phase voltage can be seen in Figure 3.

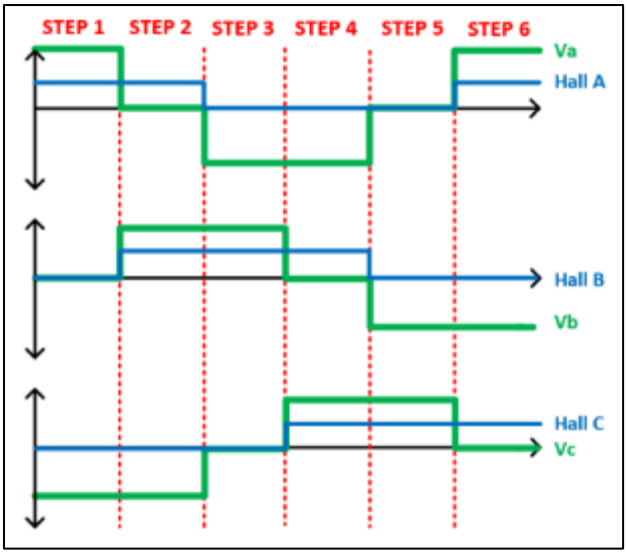

Figure 3 Timing diagram of Hall effect and phase voltage signals

2.2. Proposed Control Strategy

To get precise performance in BLDC motors, the suggested control method is to switch from regular hall effect sensors to rotary encoders. Hall effect sensors are good enough for six-step commutation, but they can only send six signal changes each electrical cycle, which limits their resolution. This restriction makes the control system less accurate, especially when it is running at low speeds. So, the system proposed a high-resolution rotary encoder that can read 2500 Pulses Per Revolution (PPR). The big increase in feedback resolution makes it possible to use a simpler control system that gives accurate speed estimates and much faster dynamic response times.

The dsPIC30F4012 microcontroller changes the data using the timer interrupt function, which uses a constant sampling time of (t_c). Whenever an interruption occurs, the microcontroller will count the number of incoming pulses (N_c). The initial step in the calculation is to determine the number of motor revolutions that occur within that sampling period, expressed as revolutions per sample (N_s). This value is obtained by dividing the number of pulses counted by the total encoder resolution, expressed as follows

$$N_s = \frac{N_c}{2500} \tag{2}$$

After obtaining the value of revolutions per sample, the actual RPM (Revolutions Per Minute) value can be calculated

$$RPM = \frac{N_c \times 60}{2500} \tag{3}$$

The integration between the high resolution of the rotary encoder and the timer interrupt on this dsPIC30F4012 allows the system to obtain RPM data in real time, which is then used as the main input parameter in the hysteresis control algorithm.

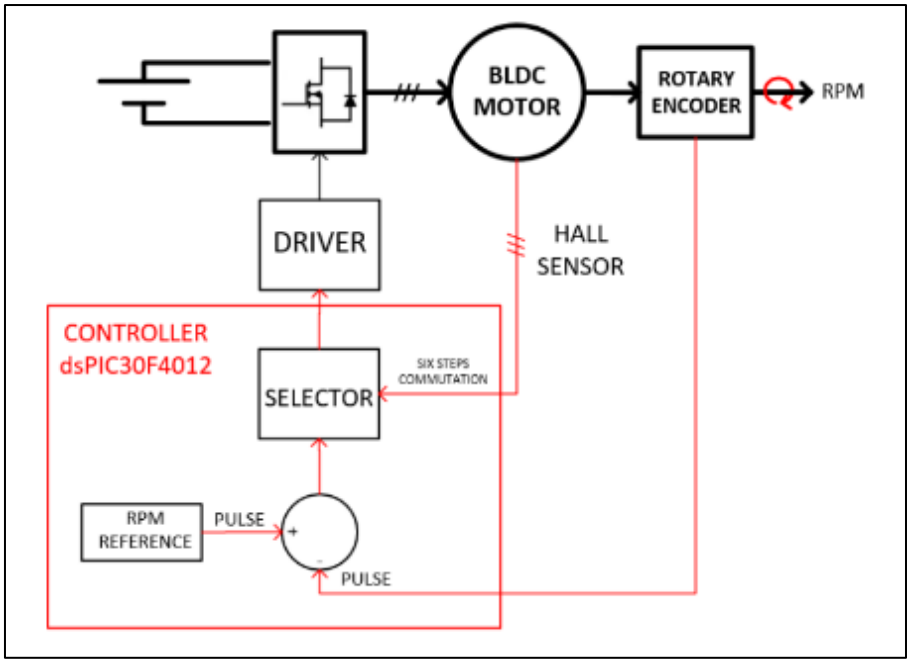

Figure 4 Schematic diagram of the proposed control system

The overall control system is shown in Figure 4. Based on the block diagram, the system works by comparing the pulse feedback value against the reference value. In order for the comparator block to compare them, the RPM Reference input value must first be converted into pulse units. The reference pulse value (*REF*) is determined by modifying Equation (3), resulting in the following relationship

$$REF = \frac{RPM_{ref} \times 2500}{60} \quad (4)$$

This pulse reference value is compared to the actual pulse count from the rotary encoder to generate an error signal. The generated error signal is then passed to the Selector block. To replace the hall effect sensor with a rotary encoder, both need to be calibrated, resulting in the display shown in Table 2.

Table 2 Correlation between Hall effect sensor and encoder pulse counts within each BLDC motor commutation step

STEP	HALL EFFECT	ENCODER POSITION 1 (PULSE)	ENCODER POSITION 2 (PULSE)	ENCODER POSITION 3 (PULSE)	ENCODER POSITION 4 (PULSE)
1	1 0 0	0 – 104	625 – 729	1250 – 1354	1875 – 1979
2	1 1 0	105 – 208	730 – 833	1355 – 1458	1980 – 2083
3	0 1 0	209 – 312	834 – 937	1459 – 1562	2084 – 2187
4	0 1 1	313 – 416	938 – 1041	1563 – 1666	2188 – 2291
5	0 0 1	417 – 520	1042 – 1145	1667 – 1770	2292 – 2395
6	1 0 1	521 – 624	1146 - 1249	1771 – 1874	2396 – 2500

The relationship between the mechanical cycle and the electrical cycle is determined by the number of magnetic pole pairs (P) on the rotor. In this case, one full mechanical rotation ($\theta_m = 360°$) consists of four electrical cycles (θ_e) generated by the four-pole configuration on the rotor. So, the relationship between the angles is

$$\theta_e = P \times \theta_m \quad (5)$$

To determine the number of pulses in one electrical cycle (90°) is

$$PPR_e = \frac{2500}{P} \quad (6)$$

Referring to Equations (5) and (6), it is obtained that one electrical cycle has a capacity of 625 pulses. Since it still uses a hall sensor, the electrical cycle is further divided into six-phase commutation steps. This division results in a segmentation where each commutation step has a specific pulse weight, as shown in Table 2 as a reference for the Selector block. This division structure allows the Controller to map pulse-based error signals into each phase commutation stage, thus maintaining synchronization between rotor position and motor speed.

Figure 5 shows how this pulse data is used to make the speed control algorithm work. After the system is initialized, the microcontroller enters the main control loop, which runs continuously. Initially, the rotary encoder transmits a pulse to acquire real-time data regarding the rotor's position.

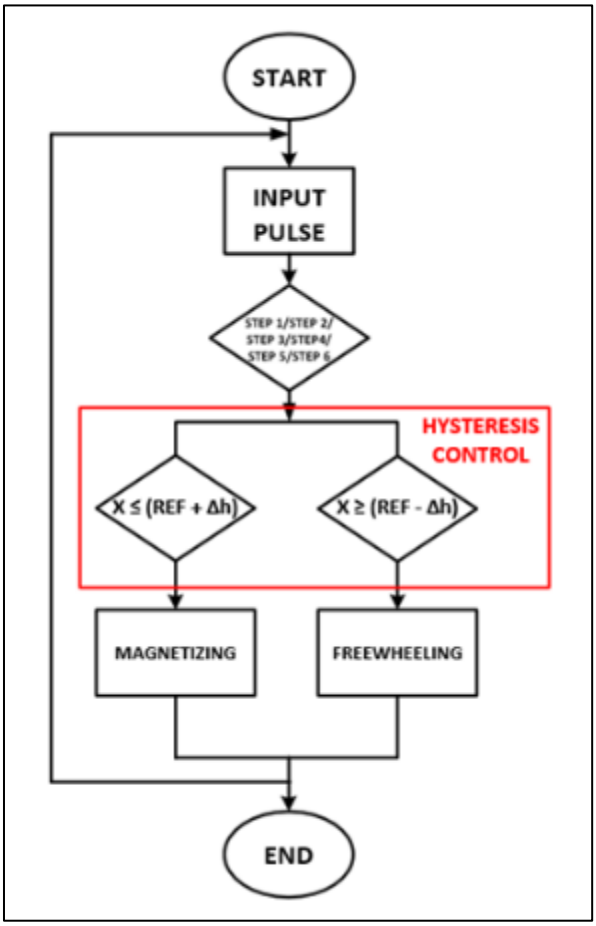

Figure 5 Algorithm of the proposed control strategy

Based on the pulse value read, the algorithm will immediately determine the motor's current position in which step (between step 1 and step 6) according to the division explained in Table 2. After the step position is known, the control logic continues to compare the actual pulse value (X) with the reference value (REF). At this point, the role of Delta (Δh) is as a threshold value or hysteresis band. The Delta used in this system is five. If the error exceeds that threshold value, the algorithm will decide whether the system needs to perform a magnetizing or freewheeling process. Figure 6 shows the equivalent circuits for magnetizing and freewheeling modes. The equation for the upper threshold in a hysteresis system is expressed as

$$X \leq (REF + \Delta h) \quad (7)$$

And the lower threshold equation in hysteresis is obtained as follows

$$X \geq (REF - \Delta h) \quad (8)$$

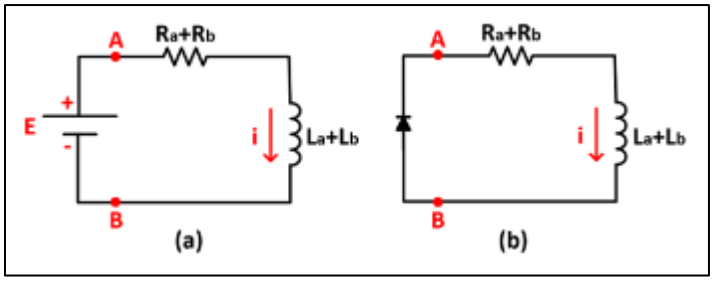

Figure 6 Equivalent circuit of (a) magnetizing mode and (b) freewheeling mode

If the actual value satisfies Equation (7), the algorithm will instruct the system to perform the magnetizing process. Applying voltage to the motor coil will trigger the appearance of induced electromotive force (E), according to the equation

$$E = L\frac{di}{dt} \tag{9}$$

This magnetizing process results in a gradual increase in electric current, which then generates electromagnetic torque or motor torque (T_m). The relationship between the torque difference and the motor's mechanical response is expressed as

$$T_m - T_l = J\frac{d\omega}{dt} \tag{10}$$

To increase the motor speed to the setpoint value, the system is designed so that the motor torque generated is greater than the load torque ($T_m > T_l$). This condition results in positive angular acceleration ($\frac{d\omega}{dt} > 0$), causing the actual pulse value (X) to increase until it reaches the upper reference threshold.

When the actual value is equal to Equation (8), freewheeling mode happens. At this point, the voltage source is turned off, which makes the current in the coil go down. Equation (9) shows how the self-induced electromotive force lets go of stored magnetic energy. The induced electromotive force (E) will decrease until it reaches zero. This drop causes the motor torque to drop to a level where ($T_m < T_l$). Equation (10) shows that this situation results in a negative angular acceleration ($\frac{d\omega}{dt} < 0$), which causes the actual pulse value (X) to drop toward a lower reference threshold. This cycle happens quickly and repeatedly, which keeps the speed of the BLDC motor within the hysteresis band.

3. Results and discussion

A simulation was conducted prior to testing the prototype. This phase was to verify the efficacy of the developed control algorithm to confirm the system's operational reliability. The outcomes of this simulation functioned as a benchmark and parameter standard for practical prototype evaluation.

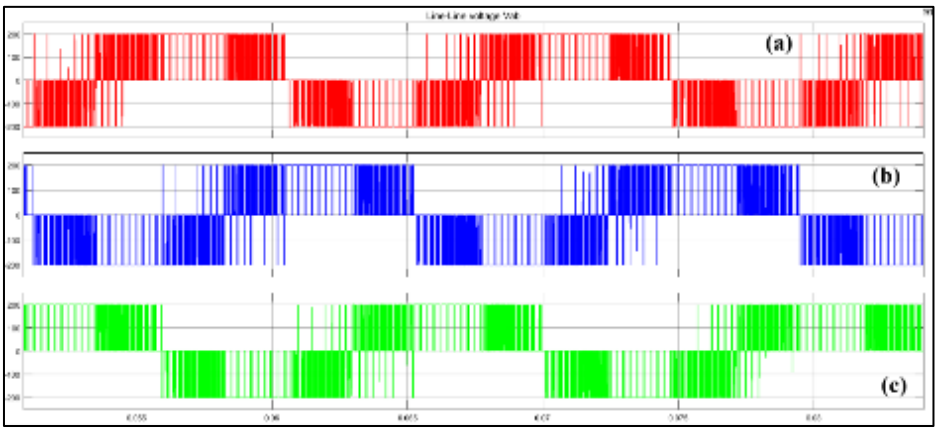

Figure 7 Simulation result of BLDC motor line-to-line voltages : (a) V_{ab}, (b) V_{bc}, and (c) V_{ca}

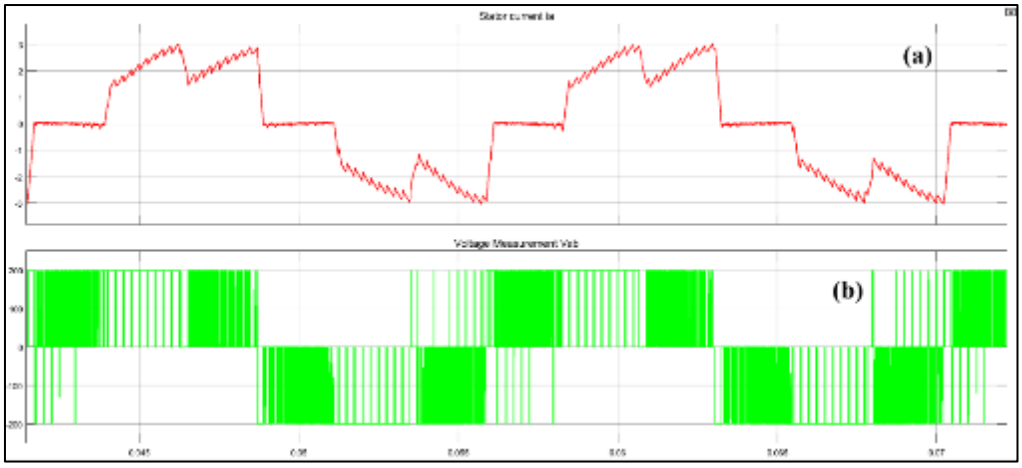

Figure 8 Comparison between (a) i_a and (b) V_{ab}

The first and second simulations are shown in Figure 7 and Figure 8. The results of the first simulation show that the phase-to-phase voltage outputs V_{ab}, V_{bc}, and V_{ca} have shifted by 120°. Meanwhile, the second simulation shows a comparison between phase A current (i_a) and voltage V_{ab}.

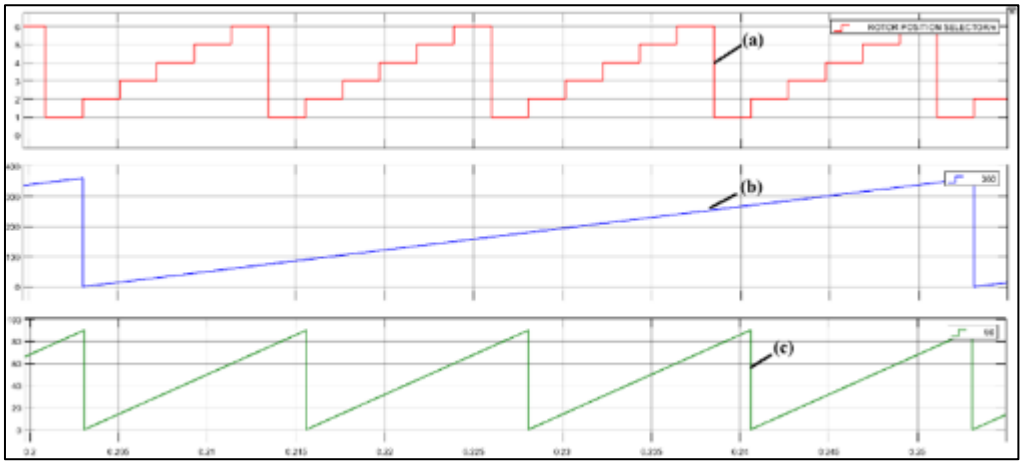

Figure 9 Comparison of simulation domains: (a) rotor position selector, (b) 360° mechanical rotation, and (c) 90° electrical rotation

Figure 9 illustrates the results of the simulation, which show how the BLDC motor's mechanical and electrical sections interact. The red signal (a) shows the six-step commutation signal from the Hall effect sensor, where one full cycle defines one electrical revolution. The blue signal (b) represents the mechanical position of the rotor, where one cycle equals one mechanical revolution. The green signal (c) shows the 90° electrical angle signal. It can be seen that during one full mechanical revolution (blue signal), the six-step commutation signal (red signal) completes exactly four full cycles of electrical revolutions (green signal). This relationship confirms that the motor has a 4:1 ratio between electrical and mechanical rotations.

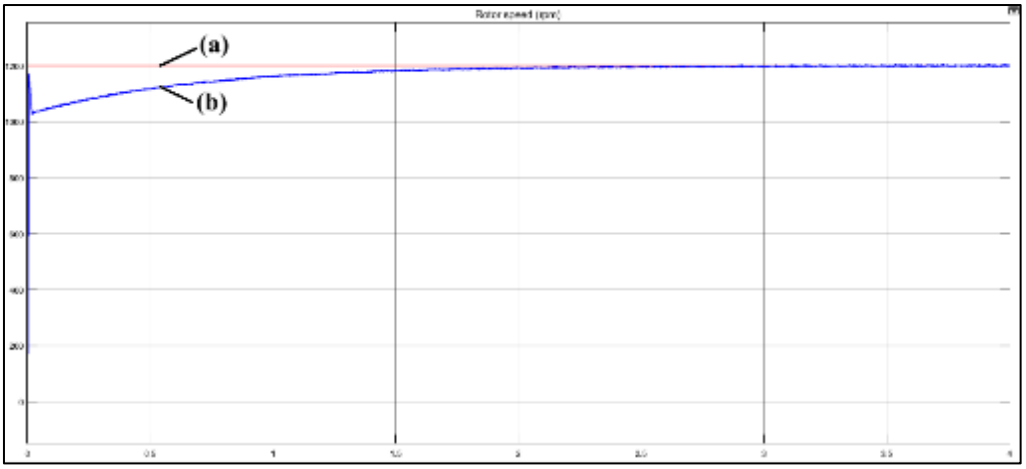

(a)

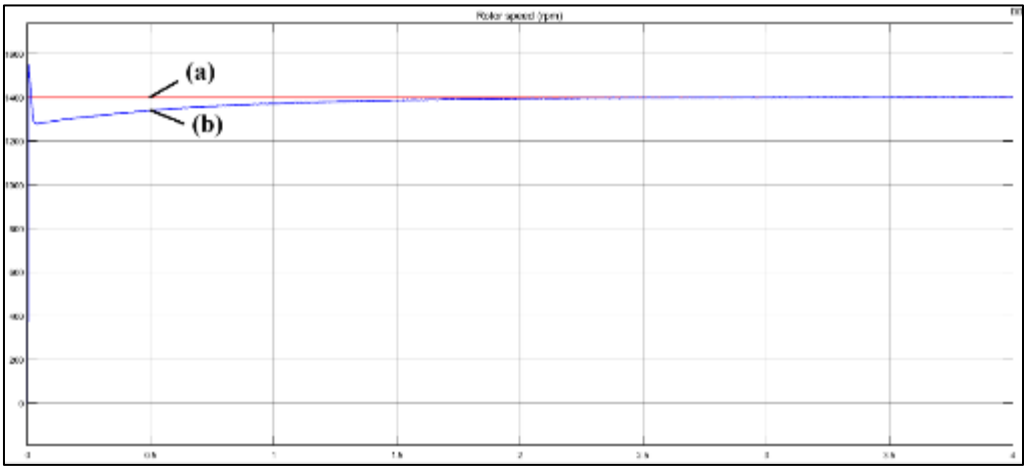

(b)

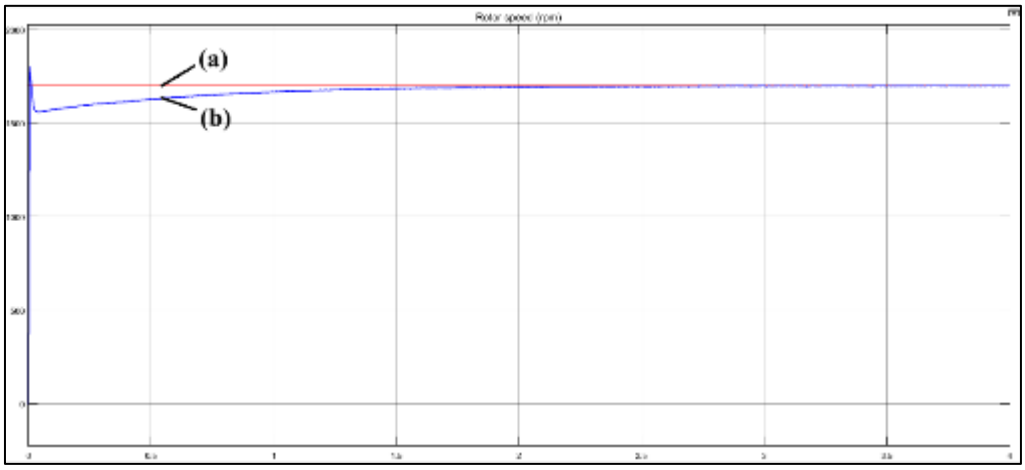

(c)

Figure 10 Simulation results of the BLDC motor hysteresis control based on reference setpoint (a) 1200 RPM, (b) 1400 RPM, and (c) 1700 RPM

Figure 10 shows the graph of motor speed (RPM) response against the setpoint reference value. The red line (a) represents the setpoint value, while the blue line (b) shows the actual motor speed. It can be seen that the hysteresis control system is able to work well and successfully lock the motor speed at various setpoints.

The simulation results were validated by conducting laboratory-scale testing. This test was conducted using a prototype designed as shown in Figure 11. The prototype tool consists of (a) a battery to supply the driver, (b) a dsPIC30F4012 microcontroller, (c) a three-phase inverter, (d) a BLDC motor, (e) a rotary encoder, (f) a tachometer, (g) a power supply, and (h) an oscilloscope. The specifications of the motor used can be seen in Table 3.

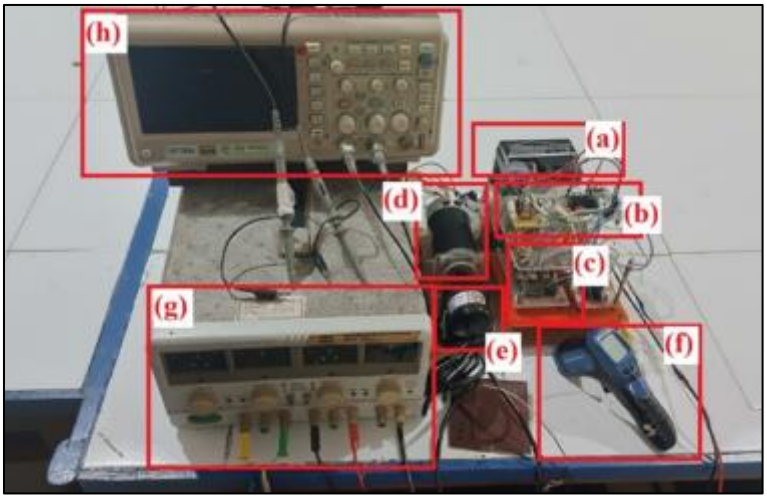

Figure 11 The prototype for experimental works

Table 3 BLDC motor specification

Parameter	Value	Unit
Nominal Voltage	24	VDC
Number of poles	8	Poles
Number of phases	3	Phases
Rated torque	0.063	N.m
Rated speed	4000	RPM
Rated current	1.9	Amps

Testing was conducted by applying a system supply voltage of 24V DC and setting the pulse reference (setpoint) at 80, 100, and 120 using hysteresis control with $\Delta h = 5$. Documentation of the test results on the oscilloscope and the tachometer display for each reference input can be seen in Figures 12 – 15.

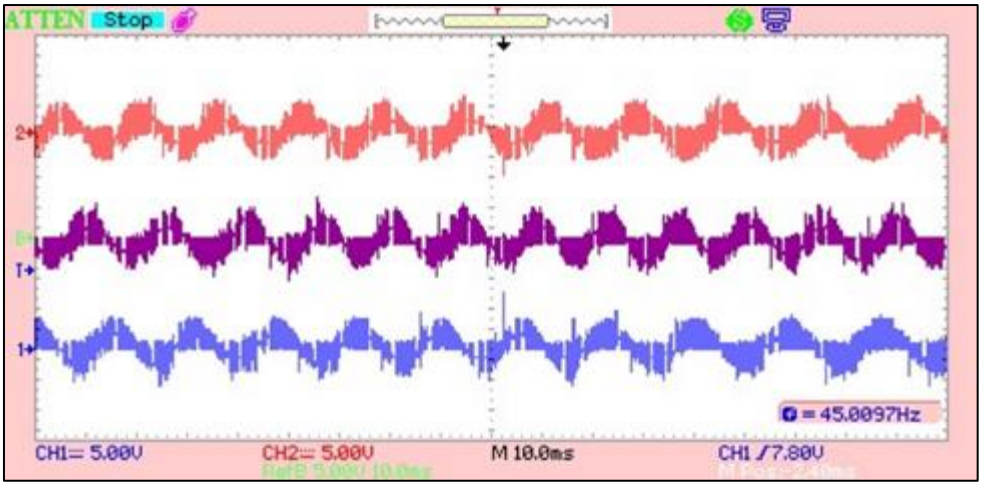

Figure 12 Experimental result of BLDC motor line-to-line voltages: (a) V_{ab}, (b) V_{bc}, and (c) V_{ca}

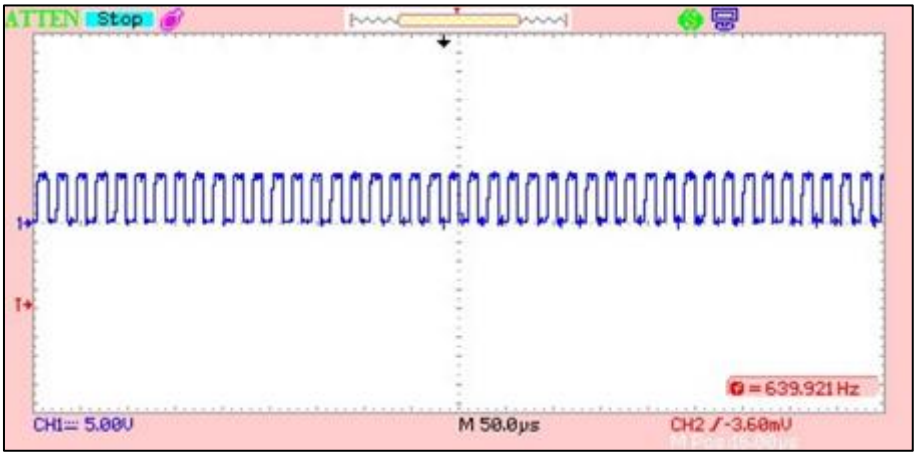

(a)

(b)

Figure 13 Experimental result of BLDC motor speed control based on a reference pulse input of 80: (a) encoder pulse signals and (b) tachometer measurement

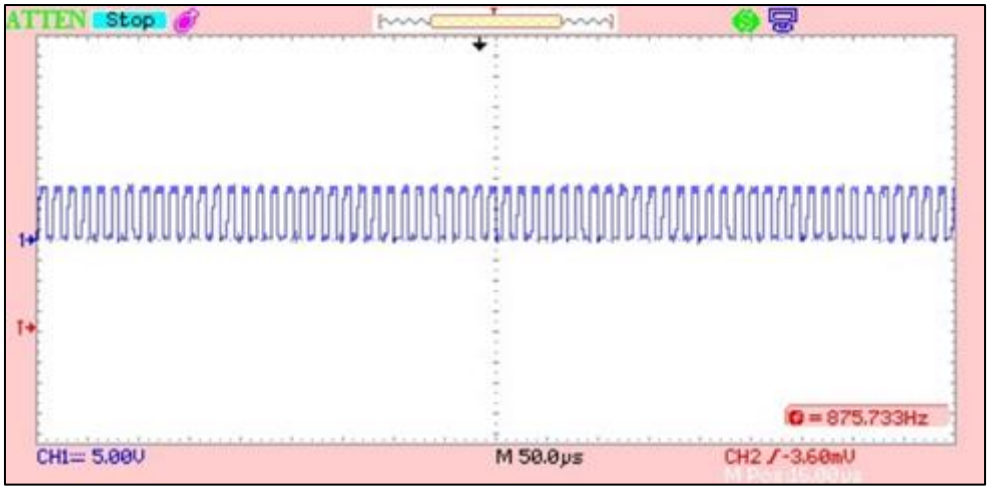

(a)

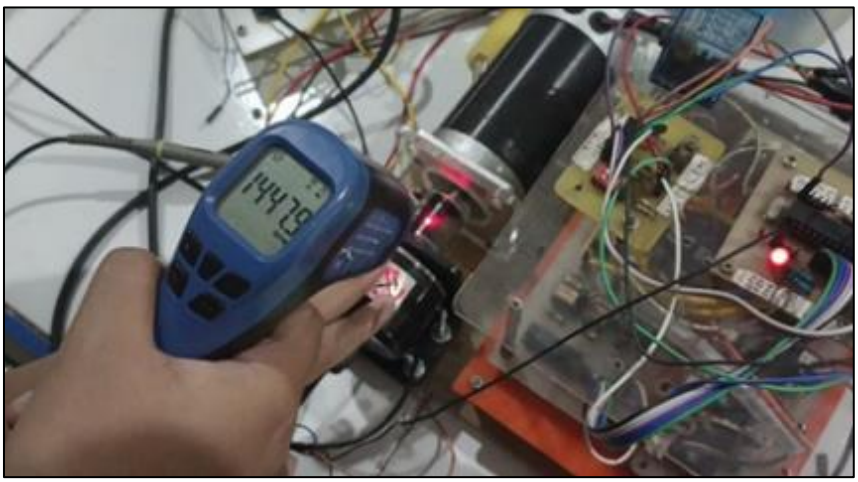

(b)

Figure 14 Experimental result of BLDC motor speed control based on a reference pulse input of 100: (a) encoder pulse signals and (b) tachometer measurement

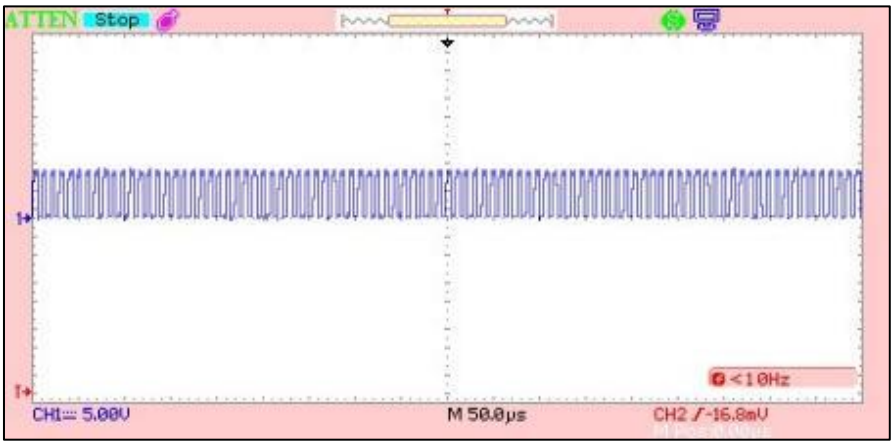

(a)

(b)

Figure 15 Experimental result of BLDC motor speed control based on a reference pulse input of 120: (a) encoder pulse signals and (b) tachometer measurement

Based on the oscilloscope display, the pulse signal generated by the rotary encoder provides real-time data about the number of pulses on each reference input used. The motor speed is calculated based on pulse data captured through an oscilloscope. By analyzing these pulse signals, the actual motor speed can be obtained as follows

$$RPM_{meas} = \left(\frac{Number\ of\ Pulses}{Number\ of\ Divisions \times Time\ per\ Division}\right) \times 60 \qquad (11)$$

To validate the accuracy of the calculation method used, the results of the calculation were subsequently compared with the speed values obtained directly from a tachometer. Table 4 summarizes the details of the conducted testing data.

Table 4 Experimental results of pulse and RPM measurement

No.	Reference Pulse/90µs	Actual Pulse/90µs	Calculated RPM	Measured RPM (Tachometer)
1	80	81	1200	1264,1
2	100	99	1466,6	1447,9
3	120	117	1733,3	1723,2

4. Conclusion

The findings of this study indicate that the dsPIC30F4012 microcontroller effectively regulated the speed of the BLDC motor. The system always locked the actual speed to the target speed under three test conditions and reference pulse values of 80, 100, and 120, which were equal to speeds of 1200 RPM, 1467 RPM, and 1733 RPM. It is clear that hysteresis control does an excellent job of maintaining the motor's spin stability at all setpoints. The feedback from the rotary encoder helps the device switch between magnetizing and freewheeling quickly. The results of these three tests are what the simulation model said they would be. This means that the control system that was designed is correct and works well at both low and high speeds, and can be used in a lot of real-life situations.

Compliance with ethical standards

Disclosure of conflict of interest

No conflict of interest to be disclosed.

References

[1] L. G. Ronauly and S. Riyadi, "A BLDC Motor Control with Variable Excitation Angle to Obtain Optimum Torque," in *2019 International Conference on Electrical Engineering and Informatics (ICEEI)*, Bandung, Indonesia: IEEE, Jul. 2019, pp. 330–335. doi: 10.1109/ICEEI47359.2019.8988897.

[2] H. Nabil, "Position Estimation and Control of BLDC motor Based on Hall effect sensor and Angular Magnetic Encoder IC," vol. 5, no. 1, 2018.

[3] G. Gupta and M. Sreejeth, "Comparative analysis of Speed control of BLDC motor using PWM and Current Control Techniques," in *2022 IEEE IAS Global Conference on Emerging Technologies (GlobConET)*, Arad, Romania: IEEE, May 2022, pp. 610–614. doi: 10.1109/GlobConET53749.2022.9872173.

[4] Uk-Youl Huh, Je-Hie Lee, and Tae-Gyoo Lee, "A torque control strategy of brushless DC motor with low resolution encoder," in *Proceedings of 1995 International Conference on Power Electronics and Drive Systems. PEDS 95*, Singapore: IEEE, 1995, pp. 496–501. doi: 10.1109/PEDS.1995.404872.

[5] U. K. Soni and R. K. Tripathi, "Recent Challenges and Advances in the Sensorless Commutation of Brushless DC Motors," *Recent Adv. Electr. Electron. Eng. Former. Recent Pat. Electr. Electron. Eng.*, vol. 14, no. 1, pp. 90–113, Jan. 2021, doi: 10.2174/2352096513999200825105724.

[6] H. Suryoatmojo, F. G. Cladella, V. Lystianingrum, D. C. Riawan, R. Mardiyanto, and D. Ariana, "Performance of BLDC Motor Speed Control Based on Hysteresis Current Control Mechanism," in *2018 International Seminar on Intelligent Technology and Its Applications (ISITIA)*, Bali, Indonesia: IEEE, Aug. 2018, pp. 147–152. doi: 10.1109/ISITIA.2018.8710910.

[7] J. E. Muralidhar and D. P. Varanasi, "Torque Ripple Minimization & Closed Loop Speed Control of BLDC Motor with Hysteresis Current Controller".

[8] C. L. Ku, "High-Precision Position Control of Linear Perrnanent Magnet BLDG Servo Motor for Pick and Place Application".

[9] N. B. Bahari, A. Bin Jidin, A. R. Bin Abdullah, M. N. Bin Othman, and M. B. Manap, "Modeling and simulation of torque hysteresis controller for brushless DC motor drives," in *2012 IEEE Symposium on Industrial Electronics and Applications*, Bandung, Indonesia: IEEE, Sep. 2012, pp. 152–155. doi: 10.1109/ISIEA.2012.6496618.

[10] E. Cetin, "Brushless Direct Current Motor Design and Analysis," *COJ Electron. Commun.*, vol. 2, no. 2, Sep. 2021, doi: 10.31031/COJEC.2021.02.000534.

[11] B. Ramesh, K. Chenchireddy, B. N. Reddy, B. Siddharth, C. V. Kumar, and P. Manojkumar, "Closed-loop control of BLDC motor using Hall effect sensors," *Int. J. Appl. Power Eng. IJAPE*, vol. 12, no. 3, p. 247, Jul. 2023, doi: 10.11591/ijape.v12.i3.pp247-254.

[12] D. Arifiyan and S. Riyadi, "Hardware Implementation of Sensorless BLDC Motor Control To Expand Speed Range," in *2019 International Seminar on Application for Technology of Information and Communication (iSemantic)*, Semarang, Indonesia: IEEE, Sep. 2019, pp. 476–481. doi: 10.1109/ISEMANTIC.2019.8884269.

[13] M. Baszynski and S. Pirog, "A Novel Speed Measurement Method for a High-Speed BLDC Motor Based on the Signals From the Rotor Position Sensor," *IEEE Trans. Ind. Inform.*, vol. 10, no. 1, pp. 84–91, Feb. 2014, doi: 10.1109/TII.2013.2243740.